Reviews in Mineralogy & Geochemistry
Vol. 62, pp. 169-191, 2006

Water in Natural Mantle Minerals II: Olivine, Garnet and Accessory Minerals

Anton Beran and Eugen Libowitzky

Institut für Mineralogie und Kristallographie
Universität Wien - Geozentrum
Althanstraße 14, A-1090 Wien, Austria
anton.beran@univie.ac.at *eugen.libowitzky@univie.ac.at*

INTRODUCTION

Hydrogen traces change the physical properties of mantle minerals to an extent that is far out of proportion to its low concentration. These properties include mechanical strength, melting behavior, diffusion rate, electrical conductivity, viscosity and rheology. Besides minerals of the pyroxene group (as discussed by Skogby 2006, this volume), the close-packed mineral structures of olivine, garnet and some accessory minerals offer important storage sites for hydrogen traces in the Earth's mantle. However, the water content stored in olivine and mantle garnet is quite low compared to that in pyroxenes.

Based on chemical considerations, but also on information obtained from infrared (IR) data, Martin and Donnay (1972) proposed the existence of hydroxyl in nominally anhydrous minerals (NAMS) occurring in the upper mantle, especially in pyroxene and olivine. The review articles of Bell and Rossman (1992a), Skogby (1999), and Ingrin and Skogby (2000) reveal a wide range of water contents for mantle-derived pyroxenes, olivines and garnets, which are derived from IR spectroscopic data. Fourier transform infrared (FTIR) spectroscopy provides an extremely sensitive method for detecting trace hydrogen bonded to oxygen in the structures of various NAMS (Beran 1999; Beran and Libowitzky 2003; Libowitzky and Beran 2004). As this method is not self-calibrating, attempts have been made to calibrate the IR spectra with independent absolute methods. These methods include hydrogen manometry and measurement of thermally released water in an electrolytic cell or by Karl Fischer titration. ^{1}H Magic-Angle-Spinning Nuclear Magnetic Resonance (MAS NMR), Secondary Ion Mass Spectrometry (SIMS) and Nuclear Reaction Analysis (NRA) are encouraging but experimentally demanding and expensive methods (as discussed by Rossman 2006, this volume). To overcome these problems, approximations such as that proposed by Paterson (1982) and refined by Libowitzky and Rossman (1997), attempt to provide a way to deal with the general dependence of the molar absorption coefficient on OH band positions in a more accurate way. The basis of the quantitative determination of the water content is the Beer-Lambert's law. IR absorbances A ($A = \log I_0/I$) are directly related by the molar absorption coefficient ε to the concentration c of OH groups and to the thickness t of the sample: $A = \varepsilon \cdot c \cdot t$. In optically anisotropic crystals normally the sum of absorbances measured with polarized radiation in principal axis directions of the optical indicatrix in oriented crystal sections results in accurate values which can be used for the determination of the water content (Libowitzky and Rossman 1996). In optically isotropic (cubic) crystals, e.g., garnets, the absorbance values from (un)polarized spectra must be multiplied by 3 to account for all three spatial directions (compare with Paterson's 1982 orientation factor $\gamma = 1/3$). Concentration values may be best obtained from integral absorbances A_i (in cm^{-1}). The integral absorption coefficient $\alpha_i = A_i/t$ (in cm^{-2}; t measured in cm) is then expressed by $\alpha_i = \varepsilon_i \cdot c$, where ε_i is the integral molar absorption coefficient in L·mol^{-1}·cm^{-2}. When ε_i is determined for a specific structural matrix, e.g.,

1529-6466/06/0062-0008$05.00 DOI: 10.2138/rmg.2006.62.8

for olivine or garnet of specific composition, then for all other olivines or garnets of the same composition and same type of OH defect the water content can be quantitatively determined by the relation c (in wt% H_2O) = $(\alpha_i \cdot 1.8)/(\varepsilon_i \cdot D)$, where D is the density of the mineral in g·cm^{-3} (Beran et al. 1993; Libowitzky and Beran 2004). Asimow et al. (2006) reported a method to derive accurate water contents from polarized measurements of randomly oriented grains.

OLIVINE

Basic structure and possible sites of hydrogen incorporation

The structure of olivine is best described as an approximately hexagonal close-packing of oxygen atoms with one half of the distorted octahedral interstices occupied by (Mg,Fe) atoms and one eighth of the tetrahedral interstices occupied by Si. One formula unit $(Mg,Fe)_2SiO_4$ contains two crystallographically different (Mg,Fe) sites, i.e., *M*1 on a center of symmetry, *M*2 in a mirror plane. Si is also placed in that mirror plane. Two of the three different oxygen positions, O1 and O2, are localized in a mirror plane, while the third, O3, occupies a general position. All oxygen atoms are coordinated by three (Mg,Fe) and one Si atom in a distorted tetrahedron. Thus, any possible structural OH defect is part of a full/vacant coordination tetrahedron and octahedron.

A first model for OH positions in olivine based on polarized IR spectroscopic measurements was proposed by Beran and Putnis (1983) for gem-quality crystals of hydrothermal origin from Zabargad, Egypt. This olivine is characterized by pleochroic absorption bands at ~3590, 3570, 3520, and 3230 cm^{-1}. It was suggested that $[O(OH)_3]$ and $[O_2(OH)_2]$ tetrahedra with a specific combination of hydrogen positions occur as structural elements, assuming that vacancies are on Si sites. If *M*2 site vacancies were assumed, $[SiO_3(OH)]$ and $[SiO_2(OH)_2]$ tetrahedra occur as structural elements.

Libowitzky and Beran (1995) presented a polarized IR study of a colorless near-endmember forsterite, revealing OH stretching bands (Fig. 1) predominantly in the high-energy wavenumber

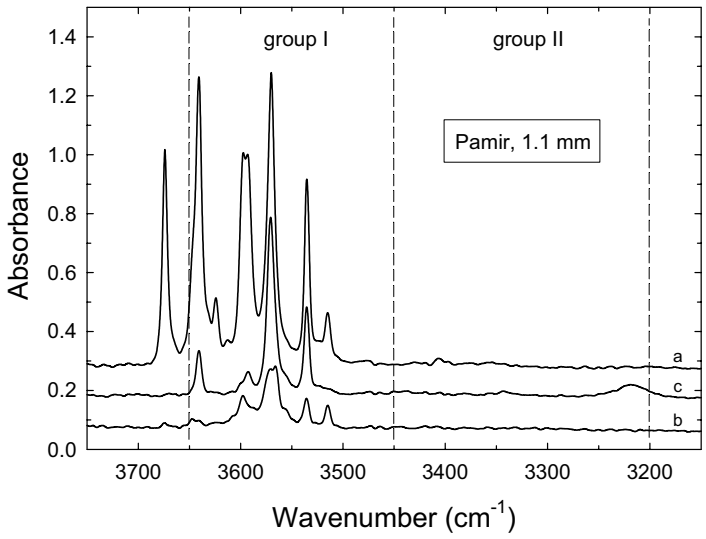

Figure 1. Polarized IR absorption spectra of an oriented forsterite crystal from a skarn deposit in Pamir, Tadzikistan, representing a crustal occurrence (Libowitzky and Beran 1995). The sharp, strongly pleochroic OH absorption bands are restricted to the high-energy region of band group I, comprising the range 3650-3450 cm^{-1}. Band group II covers the 3450-3200 cm^{-1} region (according to Bai and Kohlstedt 1993).

region (band group I according to Bai and Kohlstedt 1993). Sharp, strongly pleochroic band doublets centered at 3674/3624, 3647/3598, 3640/3592 cm^{-1} are assigned to OH dipoles oriented parallel to [100]. An OH band doublet at 3570/3535 cm^{-1} shows both, a strong absorption parallel to [100] and a strong component parallel to [001]. Under the assumption of vacancies at Si and (Mg,Fe) sites, the O1 site represents the most favorable position for OH defects pointing to a vacant Si site. O3 is proposed as donor oxygen of OH dipoles lying near the O3-O1 tetrahedral edge or roughly pointing to a vacant *M*2 site. In this model also O2 can act as donor oxygen of an OH group oriented along the O2-O3 edge of a vacant *M*1 octahedron (Fig. 2).

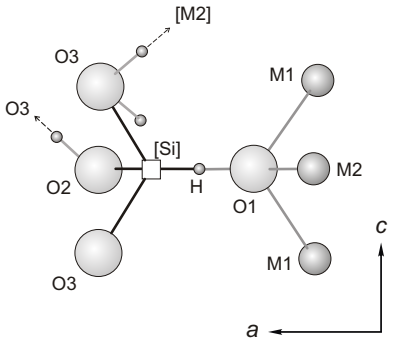

Figure 2. Schematic diagram of a part of the olivine structure with a Si vacancy showing possible OH orientations derived from the pleochroic behavior of the Pamir forsterite spectra presented in Figure 1 (modified after Libowitzky and Beran 1995).

In a recent polarized FTIR spectroscopic study of synthetic pure forsterite by Lemaire et al. (2004) the proposed OH incorporation model assuming vacant Si, *M*1, and *M*2 sites is essentially confirmed. OH bands at 3613, 3580, 3566, 3555, and 3480 cm^{-1} are assigned to OH groups compensating Si vacancies. Bands at 3600, 3220, and 3160 cm^{-1} are enhanced in samples with higher silica activity, suggesting that these bands are related to *M*1 (3160 cm^{-1}) and *M*2 vacancies (3600 and 3220 cm^{-1}). From the crystal chemical approach it is interesting to note that the predominant alignment of OH groups parallel to [100] was also observed by IR spectroscopic studies of Bauerhansl and Beran (1997) in the olivine-type mineral chrysoberyl, Al_2BeO_4.

An intense discussion of the cation vacancy type, i.e., $\square_{Mg}$ vs. $\square_{Si}$, related to hydrogen solubility was initiated on the basis of experimental results by Bai and Kohlstedt (1992, 1993). The authors carried out annealing experiments on olivine crystals from San Carlos, Arizona, with samples left unbuffered, samples buffered with orthopyroxene, and samples buffered with magnesiowustite. IR spectra from the annealed samples revealed two distinct groups of OH bands, group I bands occurred in the 3650-3450 cm^{-1} region, group II bands in the 3450-3200 cm^{-1} range. The origin of these band groups—Si vacancy and/or *M*1, *M*2 vacancies related—and their relation to *P*, *T*, silica activity, and oxygen fugacity, is still a matter of debate (Kohlstedt et al. 1996; Matveev et al. 2001, 2005; Lemaire et al. 2004; Zhao et al. 2004; Berry et al. 2005; Mosenfelder et al. 2006, and contributions in this volume, e.g., Keppler and Bolfan-Casanova 2006).

Defect types in mantle-related olivines from different localities

Based on TEM observations and IR spectroscopic investigations, Kitamura et al. (1987) described planar OH bearing defects in olivine from a kimberlite in Buell Park, Arizona. The structure of the defects resembles that of an OH bearing monolayer within the olivine structure as it exists in humite group minerals. Bands present at 3571, 3524, 3402, and possibly 3319 cm^{-1} can be assigned to titanian clinohumite. Polarized IR spectra of an olivine crystal from this locality, which contains about 50 wt ppm H_2O, have been reported by Mosenfelder et al. (2006). The strongest bands are at 3613, 3598, 3579, and 3567 cm^{-1}. The spectra of this olivine sample differ from that reported by Kitamura et al. (1987) by lack of bands due to planar titanian clinohumite defects. Two modes of hydrogen incorporation in mantle olivine from Yakutia, Siberia, were suggested by Khisina et al. (2001): Intrinsic hydrogen in form of ordered OH bearing point defects in "hydrous olivine" and extrinsic hydrogen contained in exsolutions of hydrous minerals in form of "large" inclusions. Bands observed in the olivine

spectra at 3704 and 3683 cm^{-1} can be referred to serpentine and a band at 3677 cm^{-1} to talc. The bands observed at 3591 and 3660 cm^{-1} match those of the "10 Å-phase." Lamellar and hexagon-like inclusions of several ten nm in size of Mg-vacant hydrous olivine have been described in a combined FTIR/TEM study by Khisina and Wirth (2002). Typical OH band positions of mantle-derived olivines, including the band assignment for possible planar OH bearing defects are summarized in Table 1.

Considering especially the Ti-clinohumite defects, synthetic olivines, crystallized experimentally under upper mantle conditions, that reproduce the common and intense OH bands at 3572 and 3525 cm^{-1} were reported by Berry et al. (2005). According to these authors the bands arise from OH point defects associated with traces of Ti. It should also be noted that bands at 3355 and 3325 cm^{-1} are assigned to Fe^{3+} related OH defects.

A polarized IR study of naturally occurring olivines from 17 different localities by Miller

Table 1. OH band positions (in cm^{-1}) and band assignments for possible planar OH-bearing defects for mantle olivines from different localities and occurrences.

Locality							Band assignment
1	**2**	**3**	**4**	**5**	**6**	**7**	
			3704				serpentine
		3683	3688				serpentine
3675		3676	3677				talc
		3660	3660				10 Å-phase
	3637	3637	3640	3639			serpentine
		3630		3630			
	3623	3624	3623	3624			
3610	3615	3613		3612			
3598	3602	3597	3599	3597		3599	
	3592	3591	3591	3591			10 Å-phase
3571	3576	3572	3572	3572	3572	3573	Ti-clinohumite
	3565		3562	3567	3562		
	3542	3540	3540	3541	3545		
3524	3527	3526	3526	3525	3525	3525	Ti-clinohumite
				3512			
	3499	3500					
	3481	3482		3481		3486	
	3455	3458		3458			
					3451		
	3413	3414					
3402	3400	3401					Ti-clinohumite
	3375	3374		3369			
		3355			3354		
		3330		3331	3331		
3319							Ti-clinohumite
	3298						
3230	3225						

Wavenumber values with deviations of ± 2.5 cm^{-1} are listed within one line.
1 – kimberlite xenolith, Buell Park, Arizona (Kitamura et al. 1987)
2 – kimberlite xenolith, Monastery, South Africa (Miller et al. 1987)
3 – kimberlite xenolith, Obnazennaya, Yakutia (Kishina et al. 2001)
4 – kimberlite xenolith, Udachnaya, Yakutia (Kishina et al. 2001)
5 – kimberlite xenolith, Udachnaya, Yakutia (Koch-Müller et al. 2006)
6 – spinel peridotite, Ichinomegata, Japan (Kurosawa et al. 1997)
7 – garnet peridotite, Wesselton, South Africa (Kurosawa et al. 1997)

et al. (1987) clearly demonstrated that olivines from kimberlite occurrences contain the highest hydrogen contents at a concentration level of 37-138 wt ppm H_2O (if a factor of 2.3 is applied to adjust Paterson's 1982 approximation to the recent calibration of Bell et al. 2003 - see the following chapter). The IR spectra are essentially characterized by bands in the 3600-3500 cm^{-1} high-energy and 3400-3300 cm^{-1} low-energy region. The authors also noted that over 30 distinct OH absorption bands have been identified in olivine from Monastery kimberlite, South Africa, and that the majority of these bands are inclined towards [100]. Representative polarized IR absorption spectra of olivines from South African occurrences, including olivine from Monastery, are shown in Figure 3. The presence of serpentine and talc has been determined by their characteristic OH absorption bands at 3685 and 3678 cm^{-1}, respectively (see above). Prominent OH bands at 3572 and 3525 cm^{-1} are attributed to humite group minerals (see above). Relatively uniform spectra of olivines from the Monastery kimberlite have been

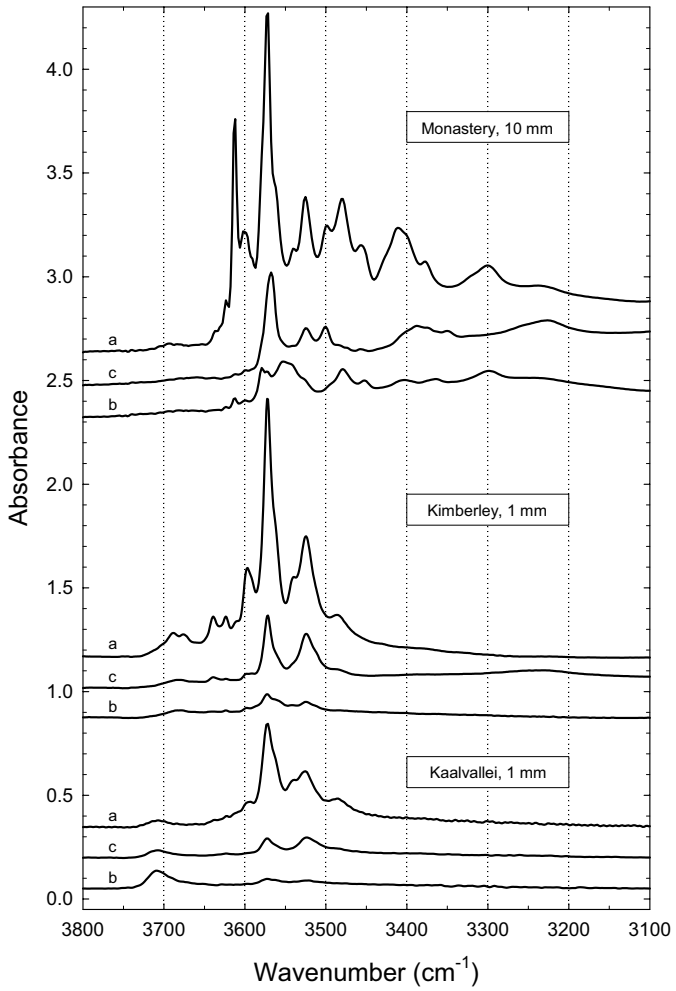

Figure 3. Representative polarized IR absorption spectra in the OH stretching frequency region of olivines from kimberlitic xenoliths of South African occurrences, indicating a preferred orientation of the OH defects parallel to *a* (modified after Miller et al. 1987 and Bell et al. 2003).

reported by Bell et al. (2004a). The olivine megacrysts represent the crystallization product of a kimberlite-like magma at pressures of about 5 GPa and temperatures of 1400-1100 °C. Spectra of olivines from the magnesian "main silicate trend" group (~13 wt% FeO) differ slightly from spectra of high-Fe olivines (17-19 wt% FeO). Both groups show a main band centered at 3572 cm^{-1} with strong polarization parallel to [100]. The high-Fe olivines are characterized by an enhanced intensity of bands at the high-energy side of the main band, and by a reduced intensity of the 3526 cm^{-1} band, relative to the main band. With respect to the OH defect assignment it is important to note that the Ti content of high-Fe olivines is significantly lower than that of low-Fe olivines. The olivines display H_2O contents in the range 45-262 wt ppm. Olivine and clinopyroxene water contents appear to increase with differentiation of the host magma, consistent with an enrichment of water in the residual melt during fractional crystallization. Inter-mineral distribution coefficients for OH between olivine and clinopyroxene are thus constant. However, the presence of strong, titanium related OH defect bands is evident.

Matsyuk and Langer (2004) published a comprehensive IR study of Yakutian upper mantle material and proposed a new nomenclature for the hydrous component in olivines. Selected IR absorption spectra, also illustrating the presence of group II bands, are shown in Figure 4. Hydroxyl groups in the form of non-intrinsic separate inclusions (NSI) were discerned from isolated local defects (ILD) or condensed extended defects (CED) intrinsic to the olivine

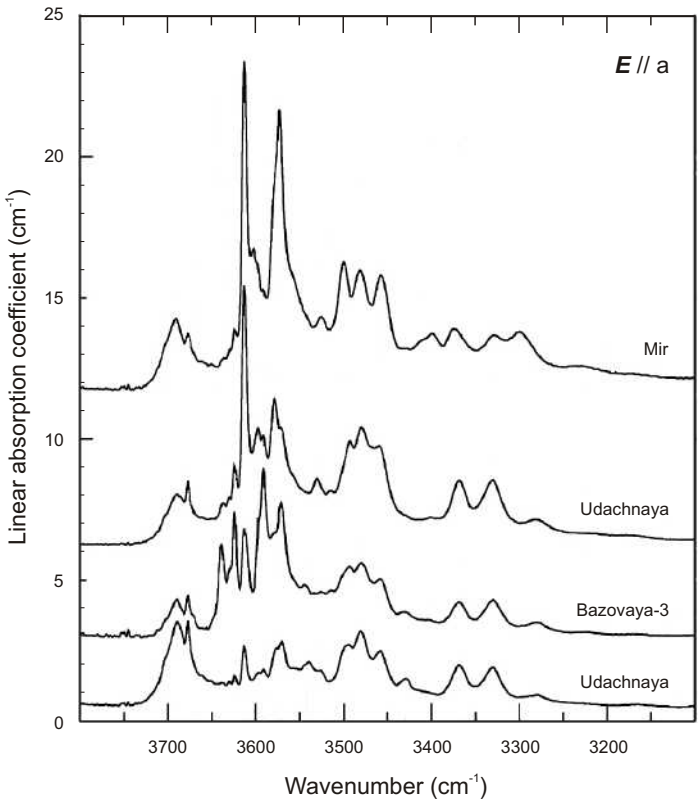

Figure 4. Selected IR absorption spectra, polarized parallel to *a*, of olivines from kimberlitic xenoliths of occurrences from the Siberian Platform, Yakutia, showing OH bands in both group I and group II regions (modified after Matsyuk and Langer 2004).

structure. As the two latter types cannot be simply distinguished by IR spectroscopy and as they are presumably interconnected by condensation reactions, it was proposed to symbolize the intrinsic defects as ILD/CED. NSI frequently comprise serpentine and talc with OH bands in the 3704-3657 cm^{-1} range (see above); Mg-edenite and Mg-pargasite occur rarely, showing bands at 3711-3709 cm^{-1}. OH stretching bands strongly polarized along [100] are a significant feature of ILD/CED. Bands in the 3570-3510 cm^{-1} region are intensity-correlated and are assigned to Si-depleted "Ti-clinohumite-like" defects (for OH-clinohumite and OH-chondrodite see Liu et al. 2003). Bands in the 3500-3300 cm^{-1} low-energy region and in the 3640-3580 cm^{-1} high-energy region are suggested to originate from OH in different types of (Mg,Fe)-depleted defects. The complex nature of the strongly polarized OH bands in the group I region is demonstrated in Figure 5. The study of Matsyuk and Langer (2004) is based on a total of 335 olivine crystal grains extracted from 174 different specimen of Yakutian upper mantle material representing all rock types occurring in kimberlites of the Siberian platform. Though there are indications that the occurrence of individual defect types is related to the genetic peculiarities of their host rocks, straight-forward and simple correlations do not exist. It is important to note that, according to Matsyuk and Langer (2004), olivine included in diamond does not contain water, detectable by IR spectroscopy, neither as NSI nor as ILD/CED. Among the rock-forming olivines, those of the ilmenite bearing specimens are highest in total water content, except for olivines from peridotites with primary phlogopite. Values of the absolute water content range from 4 to about 350 wt ppm H_2O with an average around 140 wt ppm.

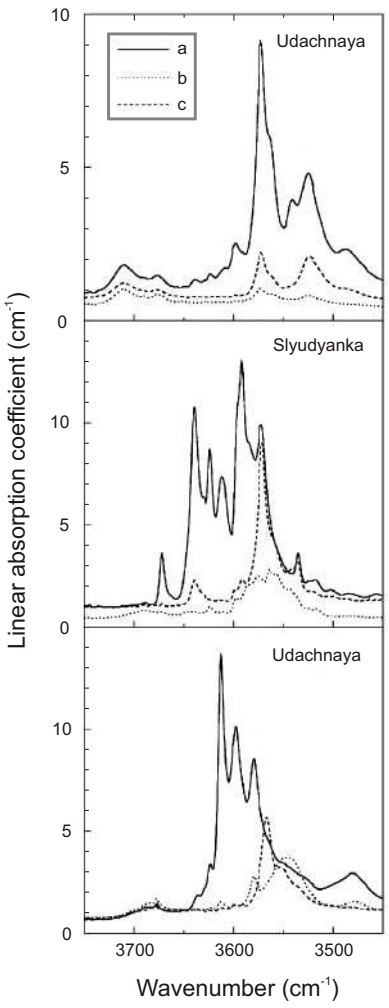

Figure 5. Polarized IR absorption spectra of olivines from kimberlitic xenoliths of Yakutian occurrences, showing the complex nature of the OH bands around 3570 cm^{-1}. The preferred orientation of the OH defects parallel to *a* is clearly indicated (modified after Matsyuk and Langer 2004).

Kurosawa et al. (1997) determined the concentration of hydrogen and other trace elements in olivines from mantle xenoliths by a combined SIMS and IR spectroscopic study. The H_2O contents are in the range of 13 to 60 wt ppm. In contrast to the observations made by Matsyuk and Langer (2004), the SIMS analyses of olivine included in diamond yielded similar hydrogen concentrations. Therefore, the authors concluded that the hydrogen content of xenolithic olivines does not equilibrate with water in the host magma during transport from the mantle to the surface. Comparing olivines from spinel peridotites with those from garnet peridotites, the presence of additional absorption bands in the band group II region (3354, 3331 cm^{-1}) is a significant feature of spinel peridotitic olivines. In garnet peridotitic olivines a positive correlation of hydrogen with the trivalent cation content (Al+Cr) was observed by

Kurosawa et al. (1997), thus indicating the incorporation of hydrogen into mantle olivines by a coupled substitution mechanism.

Light elements for a suite of ten mantle-derived olivine crystals have been measured by EMP, SIMS and FTIR spectroscopy (Kent and Rossman 2002). Li, B and H_2O concentrations are in the range of 0.9-7.8, 0.01-67, and 0.8-61 wt ppm, respectively. Although Li, B and H_2O contents vary substantially, their cation proportions are not strongly correlated, arguing against coupled substitutions.

More than 20 strongly polarized OH bands in the 3730-3330 cm^{-1} range have been reported by Koch-Müller et al. (2006) for olivine crystals from the Udachnaya kimberlite. Bands in the 3730-3670 cm^{-1} region were assigned to inclusions of serpentine, talc and "10 Å-phase." All other bands were believed to be intrinsic to the olivine structure and it was proposed that the corresponding OH point defects are associated with vacant Si and vacant *M*1 sites, i.e., O1-H defects, aligned strongly parallel to [100]. The absolute water contents range from 49 to 392 wt ppm.

Calibration approaches and summary of hydrogen contents

Though there exist older approaches to calibrate the hydrogen content in olivine, e.g., by the general diagram of Paterson (1982), only the two most recent calibration studies that end up with comparable values are reported here.

The hydrogen contents of three natural olivines determined by ^{15}N nuclear reaction analysis (NRA), i.e., 140, 220, and 16 wt ppm H_2O, were used by Bell et al. (2003) to calibrate the IR spectroscopic data for the quantitative hydrogen analysis of olivines. The OH defect concentration expressed as wt ppm H_2O is 0.188 times the total integral absorbance of the fundamental OH stretching bands, rigorously applicable to samples dominated by OH absorptions in the high-wavenumber range 3650-3450 cm^{-1}. This equals a value of the integral molar absorption coefficient $\varepsilon_i = 28450 \pm 1830$ $L \cdot mol^{-1} \cdot cm^{-2}$. A comparison of the OH concentrations determined with the Bell et al. (2003) calibration and those derived from the general Paterson (1982) trend indicates that by using polarized radiation, the Bell et al. (2003) calibration yields OH concentrations that are higher by a factor of 2.3.

Based on SIMS analyses of four olivine samples from the Udachnaya kimberlite, Koch-Müller et al. (2006) calculated the integral molar absorption coefficient to 37500 ± 5000 $L \cdot mol^{-1} \cdot cm^{-2}$. This value is by a factor of about 1.3 slightly higher than that determined by Bell et al. (2003).

Table 2 summarizes the OH concentration values of mantle olivines from different studies and geological occurrences, based on the calibration of Bell et al. (2003). In general, the scatter of data is relatively limited and ranges from a few wt ppm to maximum values of about 400 wt ppm H_2O. The mean values are roughly in the region between 100-200 wt ppm H_2O. Considering the wide variation of localities the rather homogeneous hydrogen contents of olivines are amazing. In comparison to water contents of further important mantle minerals the sequence pyroxene > olivine > garnet can be observed. On the other hand, the water contents of these natural mantle minerals are comparatively low in the light of high-*P*/*T* phases, such as wadsleyite and ringwoodite.

GARNET

Structural and spectral features

The structure of garnet group minerals is built up by alternating corner-sharing $Me^{3+}O_6$ octahedra and SiO_4 tetrahedra, forming chains parallel to the three axes of the cubic unit cell. The resulting framework contains pseudo-cubic cavities which incorporate the larger Me^{2+} cations

Table 2. Observed OH defect concentrations in mantle olivines. Mean values in parentheses.

Geological occurrence; Locality	No. of samples	OH concentration (in wt ppm H_2O)	References
Kimberlite, xenoliths; South Africa	3	37 - 138 (71)	Miller et al. (1987)
Kimberlite, xenoliths; South Africa	2	140 - 220 (180)	Bell et al. (2003)
Kimberlite, megacrysts; Monastery, South Africa	29	45 - 262 (159)	Bell et al. (2004a)
Kimberlite, xenoliths; Siberian platform	36	4 - 350 (140)	Matsyuk and Langer (2004)
Kimberlite, xenoliths; Udachnaya, Yakutia	9	49 - 392 (239)	Koch-Müller et al. (2006)
Kimberlite; Buell Park, Arizona	1	~ 50	Mosenfelder et al. (2006)

Concentration values are derived from IR spectroscopic data, calibrated against H_2O values obtained from ^{15}N Nuclear Reaction Analysis (Bell et al. 2003).

in eight-fold dodecahedral coordination. The SiO_4 tetrahedra are distorted by an amount that depends on the size of the Me^{2+} cation in the distorted pseudo-cubes, which share two opposite edges with two tetrahedra. However, the relatively rigid SiO_4 tetrahedra can accommodate to varying Me^{2+} cation sizes by a rotation which increases the size of the Me^{2+} sites and therefore the shared $Me^{3+}O_6$ octahedral edges as well. The oxygen atoms, representing possible docking sites of hydrogen, occupy only one general crystallographic site and are coordinated by one Si, one Me^{3+} and two Me^{2+} cations in the form of an almost ideal tetrahedron.

One of the well-established OH defect types is the hydrogarnet substitution (see also Libowitzky and Beran 2006, this volume), where (SiO_4) is (partially) replaced by $(OH)_4$. This substitution mode is generally observed in OH rich samples of the grossular (more often with an andradite component)-hydrogrossular series. As originally observed by Cohen-Addad et al. (1967) and by Kobayashi and Shoji (1983) the IR spectroscopic characteristics of hydrogrossulars with more than five wt% H_2O are two broad overlapping absorption bands centered around 3600 and 3660 cm^{-1} (Rossman and Aines 1991). However, these spectroscopic characteristics were generally not observed in grossular containing less than 0.3 wt% H_2O. The great variability of the IR spectra of grossular with low H_2O content suggests that the hydrogarnet substitution is not the only means of incorporating OH groups. In addition to tetrahedral sites, OH defects apparently exist in multiple other environments. Because of the optically isotropic behavior of garnets and their widely varying OH stretching frequencies, usually in the 3700-3500 cm^{-1} region, possible sites of hydrogen incorporation can only scarcely be assigned.

The anisotropic OH stretching vibrational behavior of non-cubic natural garnet crystals with compositions close to the uvarovite-grossular binary was investigated by Andrut et al. (2002). The IR absorption behavior complies with orthorhombic, monoclinic, and triclinic crystal symmetry, respectively. According to the individual pleochroic behavior of ten non-isotropic bands, six different pleochroic patterns, i.e., four band doublets and two single bands, are distinguished. For band doublets at 3559/3540, 3572/3565, and 3595/3588 cm^{-1} as well as for a single band at 3618 cm^{-1}, models for a structural OH incorporation based on the classical $(OH)_4$ hydrogarnet substitution are proposed. In contrast, for the band doublet at 3652/3602 cm^{-1} and the single band at 3640 cm^{-1}, OH defect incorporation is explained by assuming the

presence of vacancies on octahedral and dodecahedral cation positions, leading to $[SiO_3(OH)]$ tetrahedral groups. It is concluded that in garnets containing only H traces the $[SiO_3(OH)]$ substitution mode plays an essential role as OH defect incorporation mechanism. Anisotropy of OH bands for a birefringent grossular from Asbestos, Quebec, has also been reported by Rossman and Aines (1986). Based on the presence of absorption bands around 3685, 3570, and 3530 cm^{-1} of hydrothermally grown Ti-bearing pyropes, an $[(OH)_3O]$ substitution was proposed by Khomenko et al. (1994) to compensate for the higher valence of Ti^{4+} at the Al^{3+} site.

Distance-least-squares calculations were used by Lager et al. (1989) to simulate the effect of the hydrogarnet substitution on the grossular structure. Those garnets in which the shared octahedral edge is longer than the unshared can incorporate more OH. The application of these observations to other garnet compositions suggests that mantle garnets, rich in pyrope component, may contain only very limited amounts of water. Due to the presence of a relatively sharp absorption band near 3600 cm^{-1} in synthetic pyrope, Ackermann et al. (1983) proposed the hydrogarnet substitution as a possible location for water in the mantle. According to Geiger et al. (1991) OH defects in synthetic pyropes, grown from oxides are also incorporated into the structure as a hydrogarnet component, showing a characteristic absorption band at 3629 cm^{-1}. The IR spectra of pyropes, grown from a gel starting material display several absorption bands, indicating that OH substitution is not governed solely by the hydrogarnet substitution. The splitting of the 3629 cm^{-1} band at 79 K into two narrow bands centered around 3636 and 3618 cm^{-1} has been confirmed by Geiger et al. (2000) for pyrope single-crystals doped with transition elements (Co, Cr, Ni, Ti, V). The spectrum of the Ti-bearing pyrope essentially corresponds to that observed by Khomenko et al. (1994). Geiger et al. (2000) suggested that due to the presence of four OH stretching bands in Ti-bearing pyrope (3686, 3630, 3568, and 3527 cm^{-1}), additional mechanisms of OH substitution occur. In the IR spectrum of a V^{4+}-bearing pyrope the same number of bands is observed, suggesting that higher charged cations cause additional OH substitutions and increased OH concentrations in garnet. Withers et al. (1998) found that under identical conditions of high pressure and temperature the OH content of pyrope is similar to that of grossular; at $P = 3$ GPa and $T = 1000$ °C the H_2O values amount to 0.04 wt% for pyrope and to 0.02 wt% for grossular. Both garnets, pyrope and grossular, are characterized by a single band centered at 3630 and 3622 cm^{-1}, respectively, being much sharper in grossular than in pyrope.

The IR spectra of some natural pyropes appear to be different from those of synthetic samples. Observed OH band positions of garnets from mantle occurrences are summarized in Table 3. The OH spectrum of a nearly endmember natural pyrope from high-grade blueschists of Dora Maira, Western Alps, was originally described by Rossman et al. (1989). The spectrum does not resemble that of any other natural pyrope. As shown in Figure 6, the spectrum consists of four narrow bands at 3661, 3651, 3641, and 3602 cm^{-1}, forming a triplet and a single band system. If the calibration of Bell et al. (1995) is applied (see below), the estimated H_2O content is about 58 wt ppm. From high-temperature and high-pressure IR spectra, Lu and Keppler (1997) concluded that the absorption features arise from almost free OH groups in sites with different compressibility and thermal expansivity. The intensity of the high-energy triplet increases with increasing pressure (up to 10 GPa), while the intensity of the single band at 3602 cm^{-1} decreases significantly. However, Dora Maira pyrope may not be fully representative for mantle garnets.

Representative IR absorption spectra in the OH stretching frequency region of garnets from kimberlitic xenoliths are presented in Figure 7. The IR spectra of garnets rich in pyrope component from mantle-derived xenoliths of the Colorado Plateau show a broad absorption band centered around 3570 cm^{-1} with an additional weak but broad absorption around 3650 cm^{-1} (Aines and Rossman 1984a,b). The presence of broad OH bands centered around 3570 and 3670 cm^{-1} for megacrysts of pyrope from ultramafic diatremes of the Colorado Plateau containing 22-112 wt ppm H_2O was reported by Wang et al. (1996). The authors stated that pyrope crystals from the mantle may dehydrogenate during ascent and that caution should be exercised in using the OH content of natural pyrope to infer conditions of the source region.

Table 3. OH band positions (in cm^{-1}) of mantle garnets from different localities and occurrences.

Locality							Remarks
1	**2**	**3**	**4**	**5**	**6**	**7**	
3661							
3651	3650			3650			usually weak
3641							
					3630	3630	
3602							
				3590			
	3570	3570	3570				usually strong
		3512	3512				Ti-related band

Wavenumber values with deviations of ± 4 cm^{-1} are listed within one line.
1 – blueschist, Dora Maira, Italy (Lu and Keppler 1997)
2 – kimberlite, megacryst, Kaalvallei, South Africa (Bell and Rossman 1992b)
3 – kimberlite, megacryst, Lace, South Africa (Bell and Rossman 1992b)
4 – kimberlite, megacryst, Monastery, South Africa (Bell et al. 2004a)
5 – kimberlite, xenolith, Udachnaya, Yakutia (Snyder et al. 1995)
6 – eclogite, Rietfontein, South Africa (Bell and Rossman 1992b)
7 – grospydite, Zagadochnaya, Yakutia (Beran et al. 1993)

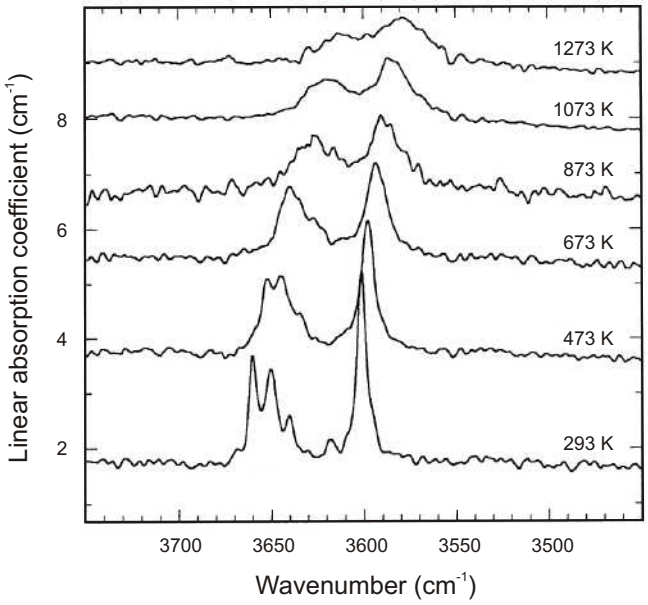

Figure 6. Room- and high-temperature IR spectra of the OH stretching vibrational region of a pyrope single-crystal from high-grade blueschists of Dora Maira, Italy (modified after Lu and Keppler 1997).

Two broad bands centered in the same wavenumber region were reported by Bell and Rossman (1992b) for pyrope-rich garnet samples from different localities of the subcontinental mantle of southern Africa (Fig. 7). A usually weak absorption centered around 3510 cm^{-1} is described as a typical feature of Ti-bearing mantle garnets (Table 3). A significant absorption at 3570 cm^{-1} for pyrope-rich garnet from the Liaoning-50 kimberlite, NE China was

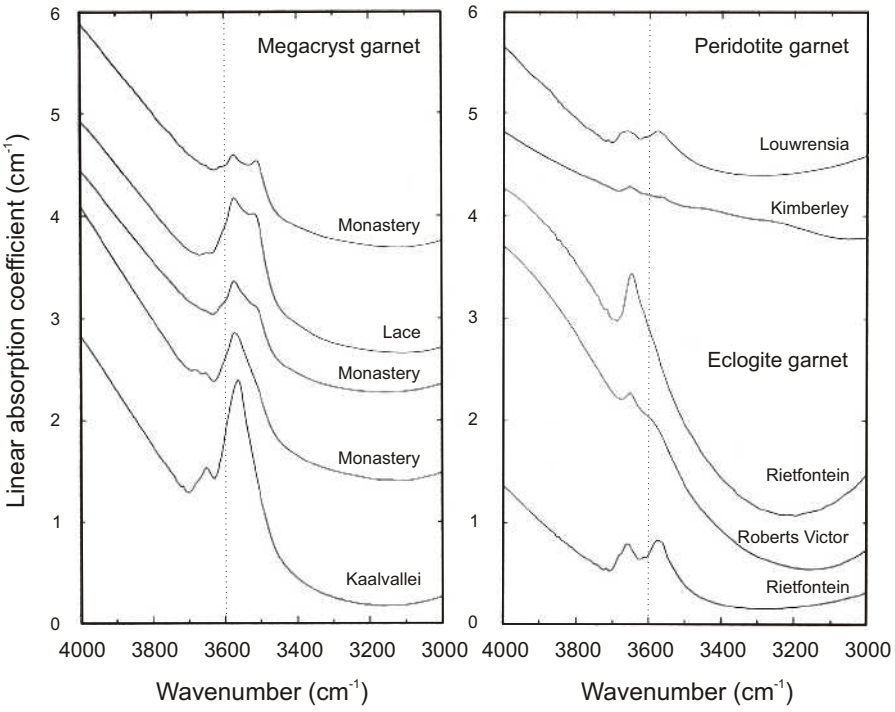

Figure 7. Representative IR absorption spectra in the OH stretching frequency region of garnets from kimberlitic xenoliths of occurrences in southern Africa. The broad absorption rising towards higher wavenumbers is due to an electronic transition of Fe^{2+} (modified after Bell and Rossman 1992b).

reported by Langer et al. (1993). Beran et al. (1993) reported a single broad absorption centered around 3630 cm^{-1} for a garnet of an eclogitic mantle xenolith from the Zagadochnaya kimberlite, Yakutia. Absorptions near 3590 and 3650 cm^{-1} are dominant in the spectra of pyrope-rich garnets from the Udachnaya kimberlite, Yakutia (Snyder et al. 1995; Table 3). A suite of 200 garnet single-crystals extracted from 150 mantle xenoliths from kimberlites of the Siberian platform was studied in the OH vibrational range by Matsyuk et al. (1998). Representative OH spectra show either one or a combination of two major bands in the 3660-3645, 3585-3560, and 3525-3515 cm^{-1} range. Bands in the latter region occur only in Ti-rich (>0.4 wt% TiO_2) garnets. Bands at 3570 and 3512 have also been reported for pyrope garnets from the Monastery kimberlite, South Africa, by Bell et al. (2004a) (Figure 7). The presence of amphibole exsolution lamellae discovered by TEM in garnets from peridotites from northern Tibet (Song et al. 2005) confirms the role of garnet as an important reservoir of water in the mantle.

Calibration and hydrogen content

Several attempts have been made to calibrate the amount of the hydrous component of garnets derived from IR spectroscopic investigations. Water contents were calculated by Aines and Rossman (1984b) by calibrating the integrated IR absorbances against the water content measured on the basis of P_2O_5 cell coulometry. ^{15}N Nuclear Reaction Analysis (NRA) has first been performed by Rossman et al. (1988) for the determination of the hydrogen content of a series of almandine, pyrope, and spessartine garnets. It was stated that pyropes contain so little hydrogen (<0.02 wt% H_2O) that satisfactory calibrations have not yet been obtained. NRA for

pyrope-almandine garnets reported by Rossman (1990) display a general positive correlation with IR peak intensity, but with considerable scatter.

Vacuum extraction and H_2 manometry has been used by Bell et al. (1995) to measure the hydrogen contents of spectroscopically characterized garnet samples of high purity and to calibrate the IR spectra for quantitative analysis. The H_2O content in the pure separates of pyrope from the Monastery kimberlite has been determined to 56 ± 6 wt ppm, resulting in an integral molar absorption coefficient of 6700 ± 670 $L \cdot mol^{-1} \cdot cm^{-2}$ (the linear molar absorption coefficient amounts to 96.9 ± 9.6 $L \cdot mol^{-1} \cdot cm^{-1}$).

A suite of 11 gem-quality garnet crystals with a broad variety of compositions were analyzed for trace amounts of hydrogen by Maldener et al. (2003) using ^{15}N NRA and FTIR microspectroscopic methods. The integral molar absorption coefficients for three pyrope-rich garnet samples with H_2O contents of 19, 17, and 18 wt ppm have been determined to 5000, 1960, and 3440 $L \cdot mol^{-1} \cdot cm^{-2}$, respectively, which would result in an average value of about 3470 $L \cdot mol^{-1} \cdot cm^{-2}$. A value of 3630 ± 1580 $L \cdot mol^{-1} \cdot cm^{-2}$ is proposed for the use in routine water determinations of compositionally different garnets, except for garnets near to endmember grossular. This value proposed by Maldener et al. (2003) is by a factor of 1.85 lower than that determined by Bell et al. (1995).

Observed OH concentrations, calibrated against the H_2O values obtained from hydrogen manometry by Bell et al. (1995) are presented in Table 4. Pyrope-rich garnets from Colorado Plateau diatremes (Green Knobs, Garnet Ridge) reported by Aines and Rossman (1984a) contain up to 260 wt ppm H_2O, garnets from the Wesselton kimberlite, South Africa, up to 70 wt ppm. OH abundances of garnets from a wide variety of rock types occurring as xenoliths in kimberlites from southern Africa (Bell and Rossman 1992b), range from less than 1 up to 135 wt ppm H_2O. A pyrope-rich garnet from the Liaoning-50 kimberlite, NE China, was reported by Langer et al. (1993) to contain about 95 wt ppm H_2O (calibrated after Maldener et al. 2003).

Table 4. Observed OH defect concentrations in mantle garnets. Mean values in parentheses.

Geological occurrence; Locality	**No. of samples**	**OH concentration (in wt ppm H_2O)**	**References**
High-grade blueschist; Dora Maira, Italy	1	58	Lu and Keppler (1997)
Ultramafic diatremes; Colorado Plateau	11	22 - 112 (59)	Wang et al. (1996)
Kimberlite, xenolith; Southern Africa	166	<1 - 135 (29)	Bell and Rossman (1992b)
Kimberlite, xenolith; Udachnaya, Yakutia	11	<1 - 72 (20)	Snyder et al. (1995)
Kimberlite, xenolith; Siberian Platform	85	<1 - 290 (70)	Matsyuk et al. (1998)
Kimberlite, megacrysts; Monastery, South Africa	19	15 - 74 (44)	Bell et al. (2004a)
Eclogite; Kokchetav, Kazakhstan	6	50 - 150 (90)	Katayama et al. (2006)
Grospydite; Zagadochnaya, Yakutia	1	620	Beran et al. (1993)

Concentration values are derived from IR spectroscopic data, calibrated against H_2O values obtained from hydrogen manometry (Bell et al. 1995).

The calibration of Bell et al. (1995) was used by Matsyuk et al. (1998) for the study of a suite of 200 garnet crystals from kimberlites of the Siberian platform, where H_2O values from below the detection limit up to maximum values of 290 wt ppm have been reported. The highest measured H_2O content of pyrope included in diamond is 36 wt ppm. The water content of most pyrope samples yields values about 70 wt ppm. According to Snyder et al. (1995) the absolute H_2O concentrations of eclogitic pyrope garnets from the Udachnaya kimberlite, Yakutia, generally cluster in the range from near 0 to 22 wt ppm, although samples occur with concentrations exceeding 70 wt ppm (Table 4). The extremely high water content of 620 wt ppm for a mantle-derived garnet from the Zagadochnaya kimberlite, Yakutia (grospydite Z 13) reported by Beran et al. (1993) is evidently related to its high grossular component ($gross_{54}pyr_{26}alm_{20}$).

The water contents of pyrope-rich garnet megacrysts reported by Bell et al. (2004a) from the Monastery kimberlite are in the range of 15-74 wt ppm H_2O and are positively correlated with Fe-enrichment—the FeO content varies between 9.5 and 14 wt%. An influence of temperature on the OH content of garnet is also suggested. OH partitioning between olivine (plus clinopyroxene) and garnet shows a factor 4-10 variation. FTIR spectroscopy and SIMS have been used by Katayama et al. (2006) to quantify trace amounts of water in pyrope-rich garnets of eclogites from the Kokchetav massif, Kazakhstan, which have been subducted to ~180 km depths. These garnets contain up to 150 wt ppm H_2O and are characterized by a single broad band with its maximum ranging from 3630 to 3580 cm^{-1}.

ACCESSORY MINERALS

Upper mantle rocks, as typically represented by peridotite and eclogite xenoliths in kimberlites, contain a range of cogenetic nominally anhydrous accessory minerals. Many of the eclogites can be argued to be crustal in origin. However, their accessories can be classified as mantle minerals since they have been subducted to mantle depths. Kyanite and rutile are probably the most abundant phases but coesite, spinel, and zircon are also included in xenoliths and present potential storage sites for hydrogen in the Earth's mantle (Rossman and Smyth 1990; Beran 1999; Libowitzky and Beran 2004).

Kyanite

The triclinic crystal structure of kyanite can be described on the basis of a distorted cubic close-packed oxygen arrangement. The aluminum cations fill 40% of the octahedral interstices in such a way that half of the occupied octahedra form single-chains parallel to the *c*-axis. The silicon atoms fill 10% of the tetrahedrally coordinated structural sites. There are two distinct silicon (Si_1, Si_2), four aluminum (Al_1-Al_4), and ten oxygen atoms (O_A-O_H, O_K and O_M) in the unit cell. Eight oxygen atoms are coordinated by one Si and two Al, two oxygen atoms (O_B and O_F), not bound to Si, are coordinated by four Al.

The recognition of OH defects in kyanite by Beran (1971) was initially based on the observation of OH absorption bands in crystals from the classical location Alpe Sponda, Switzerland. In a detailed IR spectroscopic study based on quantitative data, Beran and Götzinger (1987) established the presence of OH groups in kyanites from different geological environments, including a sample from an eclogitic xenolith in kimberlite from the Roberts Victor Mine, South Africa. OH groups in kyanites from the Roberts Victor Mine were also reported by Rossman and Smyth (1990). Beran et al. (1993) detected OH in kyanite from an eclogitic xenolith from the Zagadochnaya kimberlite, Yakutia. Two kyanites extracted by Bell et al. (2004b) from the Frank Smith kimberlite, South Africa, and from an eclogite xenolith in kimberlite from Letlhakane, Botswana, show characteristic absorption features in the OH stretching vibrational region.

According to Wieczorek et al. (2004) two main spectral types can be discerned. One type is represented by the mantle-derived kyanite from the Roberts Victor mine, consisting of a band

triplet with individual bands at 3386, 3410, and 3440 cm^{-1} of approximately equal intensities and a relatively broad low-energy band with a distinct maximum around 3275 cm^{-1}. Band deconvolution revealed a satellite band at 3260 cm^{-1}. This kyanite contains a significantly enhanced amount of Ti (0.13 wt% TiO_2). In contrast, kyanite samples from crustal rocks (and also that from the blueschists of Dora Maira) show a dominating single band at 3386 cm^{-1} and only very low intensities of the bands at 3410 and 3440 cm^{-1}. The low-energy band maxima at 3275 and 3260 cm^{-1} are clearly separated and show almost equal intensities. Both spectral types are presented in Figure 8. The pleochroic scheme of the 3386 cm^{-1} band indicates a preferred orientation of the OH dipole in the n_β' direction of the (100) cleavage plane. This orientation is in agreement with an incorporation model where O_B (not bound to Si) acts as donor oxygen of an OH group pointing directly to the centrosymmetric O_B' atom. The pleochroic behavior of the doublet band at 3275/3260 cm^{-1} is in agreement with an OH group where O_F (not bound to Si) acts as donor and O_A as acceptor oxygen (Beran 1971; Wieczorek et al. 2004).

The integral molar absorption coefficient for OH in kyanite determined by Bell et al. (2004b) on the basis of ^{15}N NRA of hydrogen amounts to 32900 $L \cdot mol^{-1} \cdot cm^{-2}$. The recalculated H_2O contents of kyanites from Roberts Victor mine, South Africa, range between 100 and 58 wt ppm (Beran and Götzinger 1987; Rossman and Smyth 1990; Wieczorek et al. 2004). The H_2O content determined by Bell et al. (2004b) for kyanite from the Letlhakane mine, Botswana, amounts to 27 wt ppm and that from the Frank Smith mine, South Africa, to 230 wt ppm. The H_2O content for the kyanite from the Zagadochnaya kimberlite, Yakutia (Beran et al. 1993), amounts to 23 wt ppm (Table 5). However, comparing the H_2O values of mantle-derived kyanites with those of kyanites from crustal occurrences (Beran and Götzinger 1987; Bell et al. 2004b; Wieczorek et al. 2004) it is evident that mantle-derived kyanites show enhanced H_2O contents. High water contents are apparently related to kyanites formed under high-*P*,*T* conditions. Finally, it should be noted that according to Wieczorek et al. (2004) kyanite from a pyrope-rutile-kyanite nodule of the blueschists from Dora Maira, Western Alps, contains 41 wt ppm H_2O.

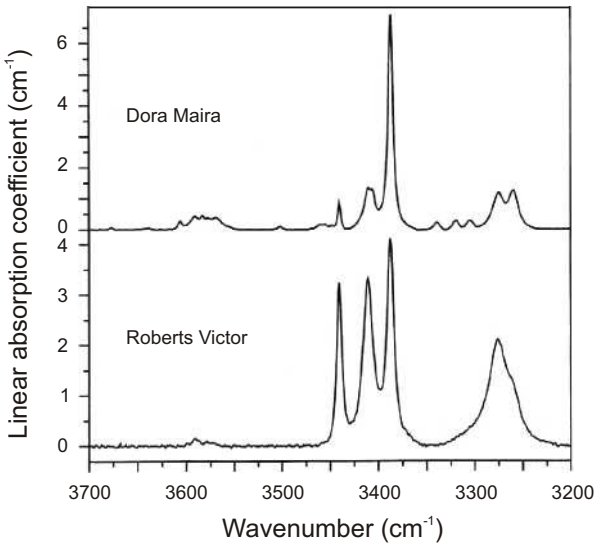

Figure 8. Polarized IR absorption spectra of two types of kyanites measured parallel to the n_β' direction in (100) sections (modified after Wieczorek et al. 2004).

Table 5. Observed OH concentrations in the accessory mantle minerals kyanite and rutile. Mean values in parentheses.

Geological occurrence; Locality	No. of samples	OH concentration (in wt ppm H_2O)	References
Kyanite			
High-grade blueschist; Dora Maira, Italy	1	41	Wieczorek et al. (2004)
Eclogitic xenolith; Roberts Victor, S.Africa	3	58 - 100 (73)	Beran and Götzinger (1987); Rossman and Smyth (1990); Wieczorek et al. (2004)
Kimberlite, xenolith; Letlhakane, Botswana	1	27	Bell et al. (2004b)
Kimberlite, xenolith; Frank Smith, S.Africa	1	230	Bell et al. (2004b)
Grospydite; Zagadochnaya, Yakutia	1	23	Beran et al. (1993)
Rutile			
High-grade blueschist; Dora Maira, Italy	1	270	Hammer and Beran (1991)
Kimberlite, xenolith; Jagersfontein, S.Africa	4	1710 - 5470 (3740)	Vlassopoulos et al. (1993)
Eclogite Kokchetav, Kazakhstan	3	330 - 740 (560)	Katayama et al. (2006)

Concentration values are derived from IR spectroscopic data, calibrated against H_2O values obtained from ^{15}N Nuclear Reaction Analysis (for kyanite see Bell et al. 2004b, for rutile Maldener et al. 2001).

Rutile

The presence of OH defects in rutile from natural occurrences was established by Beran and Zemann (1971) on the basis of strongly pleochroic absorption bands in the 3300 cm^{-1} region. Rutile as inclusion in Dora Maira pyrope, reported by Hammer and Beran (1991) is characterized by absorption bands at 3320 and 3280 cm^{-1}. A doublet of sharp bands at 3320 and 3300 cm^{-1} has been reported by Rossman and Smyth (1990) in the IR spectra of rutiles from eclogites of Roberts Victor mine, South Africa. According to Vlassopoulos et al. (1993) mantle-derived Nb- and Cr-rich rutiles from kimberlites of Jagersfontein, South Africa, are characterized by a single band centered at 3290 cm^{-1}. A single OH band at 3280 cm^{-1} has also been observed by Katayama et al. (2006) in rutile of mantle eclogites from the Kokchetav massif with corresponding H_2O contents ranging up to 740 wt ppm. Polarized spectra of this rutile sample are shown in Figure 9. From studies on synthetic material Bromiley and Hilairet (2005) concluded that the absorption band at 3279 cm^{-1}, present in the spectra of many natural samples, corresponds to OH groups that occur independently of various cation substitutions.

The OH absorption bands in rutile are strongly pleochroic, with maximum absorption perpendicular to the tetragonal *c* axis. Based on the pleochroic scheme, Beran and Zemann (1971) proposed that OH groups at the oxygen sites are oriented approximately perpendicular to the plane of the three coordinating Ti atoms. This orientation is also confirmed by the excellent agreement between expected hydrogen bond lengths calculated from band energies (~3300 → ~2.75-2.80 Å according to the d(O···O)–ν correlation of Libowitzky 1999) and

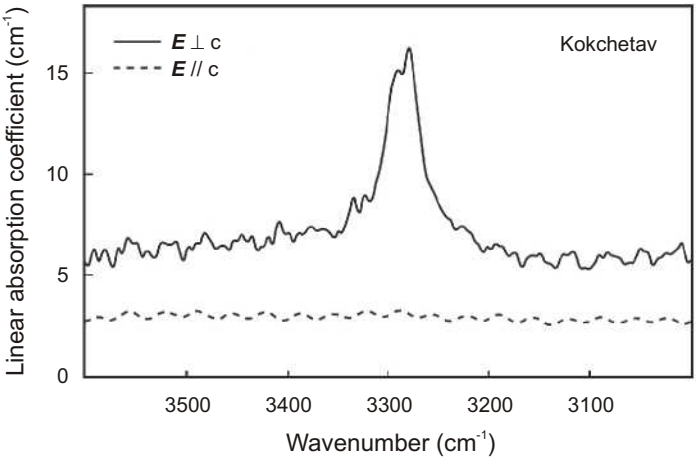

Figure 9. Polarized IR absorption spectra of accessory rutile from a mantle eclogite occurrence in Kazakhstan (modified after Katayama et al. 2006).

actually observed O···O distances of 2.78 Å. A strong deviation from this reasonable orientation has been reported by Swope et al. (1995) on the basis of neutron diffraction data obtained from an OH-rich mantle-derived rutile from Roberts Victor mine. Their proposed position of the H atom, located by examining the negative residuals in difference Fourier maps, is near to the shared edge (d(O···O) only 2.53 Å!) of the TiO_6 octahedron.

Using unpolarized radiation, but crystal plates cut parallel to c, Hammer and Beran (1991) determined the integral molar absorption coefficient for OH in rutile to 6540 $L \cdot mol^{-1} \cdot cm^{-2}$. If polarized radiation is used, Paterson's (1982) orientation factor $\gamma = 1/4$ has to be considered, resulting in a value which amounts to 26160 $L \cdot mol^{-1} \cdot cm^{-2}$. This value is based on a coulometric water determination. ^{15}N NRA has been used by Maldener et al. (2001) for the calibration of the water content in rutile from crustal occurrences, resulting in an integral molar absorption coefficient of 38000 ± 4000 $L \cdot mol^{-1} \cdot cm^{-2}$. Using this recent calibration, the H_2O content of the Dora Maira rutile (Hammer and Beran 1991) amounts to 270 wt ppm. The H_2O contents of mantle-derived rutiles from Jagersfontein, South Africa, reported by Vlassopoulos et al. (1993) range from about 1700 to 5300 wt ppm (Table 5). For comparison, maximum water contents of crustal-derived rutiles range up to about 2000 wt ppm (Hammer and Beran 1991; Vlassopoulos et al. 1993; Maldener et al. 2001), thus supporting the idea of enhanced H_2O contents in mantle-derived materials.

Structural OH groups, strongly polarized perpendicular to c, have also been reported for a number of isostructural minerals, i.e., cassiterite, SnO_2, from various localities (Beran and Zemann 1971; Maldener et al. 2001; Losos and Beran 2004), sellaite, MgF_2, from Brazil (Beran and Zemann 1985) and synthetic stishovite, the highest-pressure polymorph of SiO_2 (Pawley et al. 1993; Bolfan-Casanova et al. 2000).

Coesite

In coesite, the SiO_4 tetrahedra are connected into four-membered rings that are linked to a monoclinic framework structure which is similar to that of feldspar group minerals. The solubility of hydrogen in coesite was experimentally studied by Mosenfelder (2000). IR spectra of coesite crystals show distinct bands at 3573, 3523, 3459, and 3298 cm^{-1}. Based on Paterson's (1982) calibration, H_2O values of coesites synthesized at 1200 °C and 5-10 GPa range from 43 to 212 wt ppm. These results show that the solubility of OH in coesite is comparable to that of

pyrope-rich garnets. However, IR investigations on a variety of ultra high-pressure metamorphic rocks have failed in all cases to detect the presence of hydrogen (Mosenfelder 2000).

Koch-Müller et al. (2001) confirmed the presence of hydrogen in coesite synthesized at 3.1-7.5 GPa and 700, 800, and 1100 °C. IR spectra are characterized by three dominating bands at 3575, 3516, and 3459 cm^{-1}, two additional weak bands are centered at 3296 and 3210 cm^{-1}. Based on detailed polarized investigations, under the assumption of a vacant Si2 site the authors proposed a hydrogarnet substitution model, where O2, O3, O4, and O5 oxygen atoms are replaced by OH. Ion microprobe measurements revealed H_2O concentrations ranging from 4 to 200 wt ppm. The derived molar absorption coefficient for OH in coesite amounts to 190000 ± 30000 $L \cdot mol^{-1} \cdot cm^{-2}$. This value is by a factor of about two higher than that deduced from Paterson's (1982) diagram. Koch-Müller et al. (2003) investigated the incorporation of hydrogen into the coesite structure at pressures ranging from 4-9 GPa and temperatures from 750-1300 °C, confirming the presence of OH bands in the 3580-3450 cm^{-1} range. At 8.5 GPa and 1200 °C the hydrogen incorporation mechanism changes significantly; four bands appear at 3460, 3422, 3407, and 3379 cm^{-1} and the 3580-3450 cm^{-1} bands disappear.

Coesite from grospydites of the Roberts Victor mine, South Africa, has been described by Rossman and Smyth (1990) to contain traces of molecular H_2O, present as hydrous material residing in fractures. Based on measurements with synchrotron IR radiation, OH absorption bands in the 3600-3350 cm^{-1} region have been reported by Koch-Müller et al. (2003) in natural coesite occurring as an inclusion in diamond. The calculated H_2O content, calibrated against ion microprobe data, amounts to about 135 wt ppm. In contrast, no OH was detected in coesite by Mosenfelder et al. (2005) in pyropes from Dora Maira, though the silica phases quartz, chalcedony, and opal which surround the coesite inclusions, show considerable amounts of H_2O. Similar signatures have been observed for coesite in a grospydite xenolith from the Roberts Victor mine (Mosenfelder et al. 2005).

Spinel

Ringwoodite, the spinel polymorph of $(Mg,Fe)_2SiO_4$ likely to occur in the transition zone of the Earth's mantle can incorporate major amounts of water in form of OH groups (Bolfan-Casanova 2005; Ohtani 2005). The corresponding IR spectra are characterized by broad absorption bands centered in the 3700-3100 cm^{-1} region (Kohlstedt et al. 1996; Bolfan-Casanova et al. 2000; Kudoh et al. 2000; Ohtani et al. 2000; Smyth et al. 2003). Single-crystals of γ-Mg_2GeO_4 spinel were synthesized by Hertweck and Ingrin (2005) under hydrous conditions at 1.9 GPa and 1000 °C revealing a relatively sharp OH absorption band at 3531 cm^{-1}. The estimated H_2O content is in the order of 5-10 wt ppm. Preliminary results have been reported by Halmer et al. (2003) from highly disordered non-stoichiometric Verneuil-grown MgAl spinels. Two significant sharp bands centered at 3510 and 3355 cm^{-1} with varying band intensities are assigned to weakly hydrogen-bonded OH defects.

No indications for the presence of OH have been observed in natural aluminate ($MgAl_2O_4$-rich) spinels of mantle eclogites (Rossman and Smyth 1990). OH groups in spinels have neither been found in samples from the upper Earth's mantle nor from crustal occurrences. One may speculate whether disorder is a basic requirement for the incorporation of OH defects in the spinel structure. An additional complication results from the fact that in natural spinel samples the OH stretching vibrational region is usually overlapped by extremely strong and broad absorptions due to *d-d* transitions of tetrahedrally coordinated Fe^{2+} (Skogby and Halenius 2003), thus making the detection of trace OH a difficult task.

Zircon

Incorporation of hydrous species in natural zircon is a widely observed phenomenon. Observed water contents may range from almost zero in crystalline samples up to more than 15 wt% H_2O in radiation-damaged metamict zircons. The spectroscopy of zircon has recently

been reviewed by Nasdala et al. (2003). Whereas well-crystallized samples are characterized by sharp and strongly pleochroic OH absorption bands, metamict zircons usually display additional broad non-pleochroic IR absorption bands. The sharp bands indicate incorporation of structural OH groups and the broad bands are interpreted in terms of H_2O molecules. Narrow IR absorption bands in crystalline zircons have been described by Nasdala et al. (2001) at 3180, 3420, and 3385 cm^{-1}; the latter band is polarized perpendicular to the *c* axis, the former two are polarized parallel to *c* (Fig. 10). The 3385 cm^{-1} band is assigned to an OH group coordinated by one Si and two Zr sites, probably substituted by REE^{3+} (ZrZrSi). Assuming cation vacancies (□), the 3180 cm^{-1} band is assigned to OH coordinated by one Si and one Zr (Zr□Si), and the 3420 cm^{-1} band to OH coordinated by two Zr atoms (ZrZr□) (Fig. 11).

OH defects in a mantle-derived zircon sample from Kimberley, South Africa, were reported by Woodhead et al. (1991). The estimated H_2O content amounts to about 70 wt ppm (based on the garnet calibration published by Bell et al. 1995). The authors stated that this value presents the maximum OH content observed in crystalline zircon in comparison with a suite of 30 zircons of crustal occurrences, suggesting high activity of H_2O in the mantle. The corresponding IR spectrum is characterized by sharp and relatively strong absorption bands at 3417 and 3384 cm^{-1} and by weak bands at 3510 and 3180 cm^{-1}. Very similar spectral features are evident in the unpolarized IR spectrum of a well-ordered zircon from a Yakutian kimberlite pipe reported by Nasdala et al. (2001), showing a strong absorption band at 3420 and a weak band at 3180 cm^{-1} (Fig. 10). Bell and Rossman (1992a) reported H_2O concentrations of zircons, formed by crystallization of a magma at high pressure, which range from about 50 to 100 wt ppm. Water contents determined by Bell et al. (2004a) on zircons associated with high-Fe olivines, ilmenite and phlogopite from the Monastery kimberlite, South Africa, are in the 28-34 wt ppm range. The spectra of these zircons are characterized by two sharp pleochroic bands centered around 3420 and 3380 cm^{-1}, superimposed on a small amount of broad, featureless absorption. However, the rarity of zircon in mantle rocks renders it of minor importance for storing essential amounts of hydrogen.

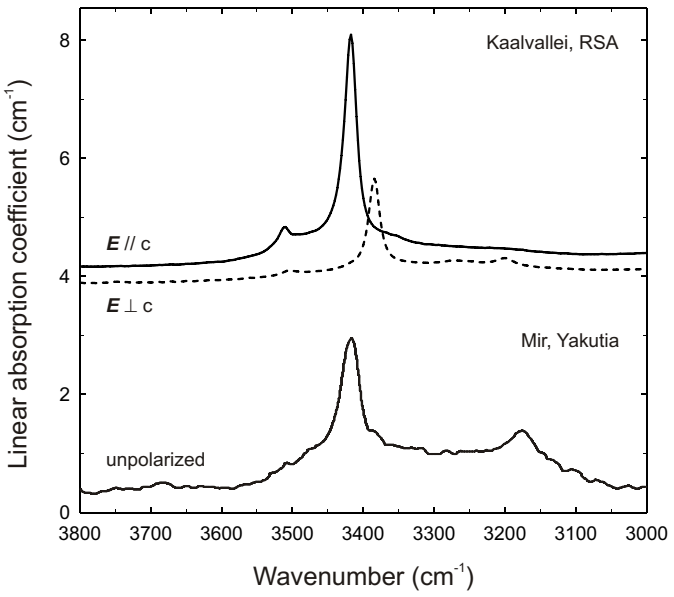

Figure 10. Characteristic IR absorption spectra of well-ordered (non-metamict) zircons from kimberlitic xenoliths (modified after Bell and Rossman 1992a, Nasdala et al. 2001).

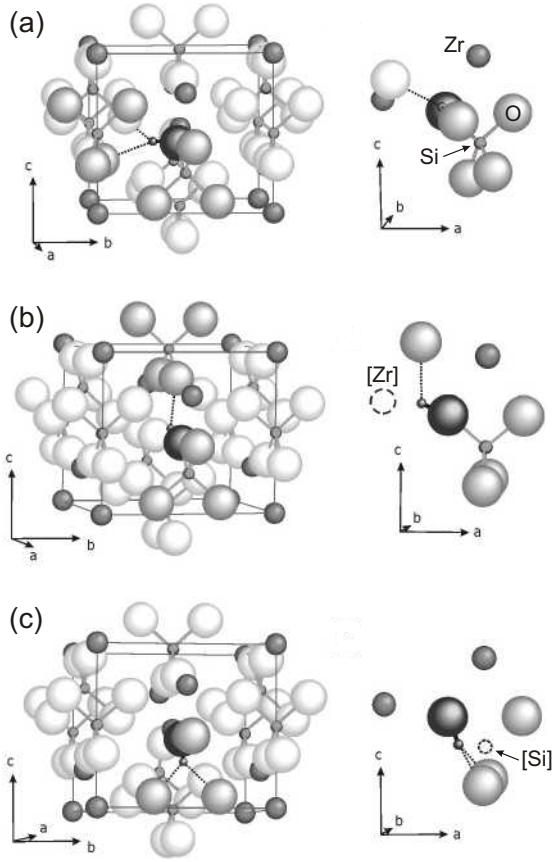

Figure 11. Potential locations of OH defects in crystalline zircon from kimberlitic xenoliths, coordinated by (a) Zr, Zr, Si, (b) Zr, $\square_{Zr}$, Si, (c) Zr, Zr, $\square_{Si}$ (modified after Nasdala et al. 2001).

ACKNOWLEDGMENTS

The authors wish to thank H. Keppler and J. Smyth for the invitation to contribute to the present MSA volume. H. Keppler, J.L. Mosenfelder and an anonymous referee helped to improve the quality of the manuscript. The topics of this paper were partly sponsored by the European Commission, Human Potential-Research Training Network, HPRN-CT-2000-0056.

REFERENCES

Ackermann L, Cemic L, Langer K (1983) Hydrogarnet substitution in pyrope: a possible location for "water" in the mantle. Earth Planet Sci Lett 62:208-214

Aines RD, Rossman GR (1984a) Water content of mantle garnets. Geology 12:720-723

Aines RD, Rossman GR (1984b) The hydrous component in garnets: pyralspites. Am Mineral 69:1116-1126

Andrut M, Wildner M, Beran A (2002) The crystal chemistry of birefringent natural uvarovites. Part IV. OH defect incorporation mechanisms in non-cubic garnets derived from polarized IR spectroscopy. Eur J Mineral 14:1019-1026

Asimow PD, Stein LC, Mosenfelder JL, Rossman GR (2006) Quantitative polarized infrared analysis of trace OH in populations of randomly oriented mineral grains. Am Mineral 91:278-284

Bai Q, Kohlstedt DL (1992) Substantial hydrogen solubility in olivine and implications for water storage in the mantle. Nature 357:672-674

Bai Q, Kohlstedt DL (1993) Effects of chemical environment on the solubility and incorporation mechanism for hydrogen in olivine. Phys Chem Minerals 19:460-471

Bauerhansl P, Beran A (1997) Trace hydrogen in the olivine-type minerals chrysoberyl, Al_2BeO_4 and sinhalite, $MgAlBO_4$ - a polarized FTIR spectroscopic study. Schweiz Min Petr Mitt 77:131-136

Bell DR, Rossman GR (1992a) Water in Earth's mantle: The role of nominally anhydrous minerals. Science 255:1391-1397

Bell DR, Rossman GR (1992b) The distribution of hydroxyl in garnets from the subcontinental mantle of southern Africa. Contrib Mineral Petrol 111:161-178

Bell DR, Ihiniger PD, Rossman GR (1995) Quantitative analysis of trace OH in garnet and pyroxenes. Am Mineral 80:465-474

Bell DR, Rossman GR, Maldener J, Endisch D, Rauch F (2003) Hydroxide in olivine: A quantitative determination of the absolute amount and calibration of the IR spectrum. J Geophys Res 108, B2:2105-2113

Bell DR, Rossman GR, Moore RO (2004a) Abundance and partitioning of OH in a high-pressure magmatic system: Megacrysts from the Monastery kimberlite, South Africa. J Petrol 45:1539-1564

Bell DR, Rossman GR, Maldener J, Endisch D, Rauch F (2004b) Hydroxide in kyanite: A quantitative determination of the absolute amount and calibration of the IR spectrum. Am Mineral 89:998-1003

Beran A (1971) Messung des Ultrarot-Pleochroismus von Mineralen XII. Der Pleochroismus der OH-Streckfrequenz in Disthen. Tschermaks Min Petr Mitt 16:129-135

Beran A (1999) Contribution of IR spectroscopy to the problem of water in the Earth's mantle. *In:* Microscopic Properties and Processes in Minerals. Wright K, Catlow R (eds) NATO Science Series. Kluwer Acad. Publishers, p 523-538

Beran A, Götzinger MA (1987) The quantitative IR spectroscopic determination of structural OH groups in kyanites. Mineral Petrol 36:41-49

Beran A, Libowitzky E (2003) IR spectroscopic characterization of OH defects in mineral phases. Phase Trans 76:1-15

Beran A, Putnis A (1983) A model of the OH positions in olivine, derived from infrared-spectroscopic investigations. Phys Chem Minerals 9:57-60

Beran A, Zemann J (1971) Messung des Ultrarot-Pleochroismus von Mineralen. XI. Der Pleochroismus der OH-Streckfrequenz in Rutil, Anatas, Brookit und Cassiterit. Tschermaks Min Petr Mitt 15:71-80

Beran A, Zemann J (1985) Polarized absorption spectra of sellaite from the Brumado mine, Brazil, in the near infrared. Bull Geol Soc Finlande 57:113-118

Beran A, Langer K, Andrut M (1993) Single crystal infrared spectra in the range of OH fundamentals of paragenetic garnet, omphacite and kyanite in an eclogitic mantle xenolith. Mineral Petrol 48:257-268

Berry AJ, Hermann J, O'Neill HSC, Foran GJ (2005) Fingerprinting the water site in mantle olivine. Geology 33:869-872

Bolfan-Casanova N (2005) Water in the Earth's mantle. Mineral Mag 69:229-257

Bolfan-Casanova N, Keppler H, Rubie DC (2000) Water partitioning between nominally anhydrous minerals in the MgO-SiO_2-H_2O system up to 24 GPa: implications for the distribution of water in the Earth's mantle. Earth Planet Sci Lett 182:209-221

Bromiley GD, Hilairet N (2005) Hydrogen and minor element incorporation in synthetic rutile. Mineral Mag 69:345-358

Cohen-Addad C, Ducros P, Bertaut EF (1967) Étude de la substitution du groupement SiO_4 par $(OH)_4$ dans les composés $Al_2Ca_3(OH)_{12}$ et $Al_2Ca_3(SiO_4)_{2,16}(OH)_{3,36}$ de type grenat. Acta Crystallogr 23:220-230

Geiger CA, Langer K, Bell DR, Rossman GR, Winkler B (1991) The hydroxide component in synthetic pyrope. Am Mineral 76:49-59

Geiger CA, Stahl A, Rossman GR (2000) Single-crystal IR- and UV/VIS- spectroscopic measurements on transition-metal-bearing pyrope: the incorporation of hydroxide in garnet. Eur J Mineral 12:259-271

Halmer MM, Libowitzky E, Beran A (2003) IR spectroscopic determination of OH defects in spinel group minerals. Geophys Res Abstr 5:06742

Hammer VMF, Beran A (1991) Variations in the OH concentration of rutiles from different geological environments. Mineral Petrol 45:1-9

Hertweck B, Ingrin J (2005) Hydrogen incorporation in a ringwoodite analogue: Mg_2GeO_4 spinel. Mineral Mag 69:337-343

Ingrin J, Skogby H (2000) Hydrogen in nominally anhydrous upper-mantle minerals: concentration levels and implications. Eur J Mineral 12:543-570

Katayama I, Nakashima S, Yurimoto H (2006) Water content in natural eclogite and implication for water transport into the deep upper mantle. Lithos 86:245-259

Kent AJR, Rossman GR (2002) Hydrogen, lithium, and boron in mantle-derived olivine: The role of coupled substitutions. Am Mineral 87:1432-1436

Keppler H, Bolfan-Casanova N (2006) Thermodynamics of water solubility and partitioning. Rev Mineral Geochem 62:193-230

Khisina NR, Wirth R (2002) Hydrous olivine $(Mg_{1-y}Fe^{2+}_y)_{2-x}\square_xSiO_4H_{2x}$ – a new DHMS phase of variable composition observed as nanometer-sized precipitations in mantle olivine. Phys Chem Minerals 29:98-111

Khisina NR, Wirth R, Andrut M, Ukhanov AV (2001) Extrinsic and intrinsic mode of hydrogen occurrence in natural olivines: FTIR and TEM investigation. Phys Chem Minerals 28:291-301

Khomenko VM, Langer K, Beran A, Koch-Müller M, Fehr T (1994) Titanium substitution and OH-bearing defects in hydrothermally grown pyrope crystals. Phys Chem Minerals 20:483-488

Kitamura M, Kondoh S, Morimoto N, Miller GH, Rossman GR, Putnis A (1987) Planar OH-bearing defects in mantle olivine. Nature 328:143-145

Kobayashi S, Shoji T (1983) Infrared analysis of the grossular-hydrogrossular series. Mineral J 11:331-343

Koch-Müller M, Fei Y, Hauri E, Liu Z (2001) Location and quantitative analysis of OH in coesite. Phys Chem Minerals 28:693-705

Koch-Müller M, Dera P, Fei Y, Reno B, Sobolev N, Hauri E, Wysoczanski R (2003) OH^- in synthetic and natural coesite. Am Mineral 88:1436-1445

Koch-Müller M, Matsyuk SS, Rhede D, Wirth R, Khisina N (2006) Hydroxyl in mantle olivine xenocrysts from the Udachnaya kimberlite pipe. Phys Chem Minerals 33:276-287

Kohlstedt DL, Keppler H, Rubie DC (1996) Solubility of water in the α, β and γ phases of $(Mg,Fe)_2SiO_4$. Contrib Mineral Petrol 123:345-357

Kudoh Y, Kuribayashi T, Mizobata H, Ohtani E (2000) Structure and cation disorder of hydrous ringwoodite, γ-$Mg_{1.89}Si_{0.98}H_{0.30}O_4$. Phys Chem Minerals 27:474-479

Kurosawa M, Yurimoto H, Sueno S (1997) Patterns in the hydrogen and trace element compositions of mantle olivines. Phys Chem Minerals 24:385-395

Lager GA, Armbruster T, Rotella FJ, Rossman GR (1989) OH substitution in garnets: X-ray and neutron diffraction, infrared, and geometric-modeling studies. Am Mineral 74:840-851

Langer K, Robarick E, Sobolev NV, Shatsky VS, Wang W (1993) Single-crystal spectra of garnets from diamondiferous high-pressure metamorphic rocks from Kazakhstan: indications for OH^-, H_2O, and FeTi charge transfer. Eur J Mineral 5:1091-1100

Lemaire C, Kohn SC, Brooker RA (2004) The effect of silica activity on the incorporation mechanisms of water in synthetic forsterite: a polarised infrared spectroscopic study. Contrib Mineral Petrol 147:48-57

Libowitzky E (1999) Correlation of O-H stretching frequencies and O-H···O hydrogen bond lengths in minerals. Mh Chem 130:1047-1059

Libowitzky E, Beran A (1995) OH defects in forsterite. Phys Chem Minerals 22:387-392

Libowitzky E, Beran A (2004) IR spectroscopic characterisation of hydrous species in minerals. *In*: Spectroscopic Methods in Mineralogy. Beran A, Libowitzky E (eds), EMU Notes Mineral 6, Eötvös Univ Press, p 227-279

Libowitzky E, Beran A (2006) The structure of hydrous species in nominally anhydrous minerals: information from polarized IR spectroscopy. Rev Mineral Geochem 62:29-52

Libowitzky E, Rossman GR (1996) Principles of quantitative absorbance measurements in anisotropic crystals. Phys Chem Minerals 23:319-327

Libowitzky E, Rossman GR (1997) An IR absorption calibration for water in minerals. Am Mineral 82:1111-1115

Liu Z, Lager GA, Hemley RJ, Ross NL (2003) Synchrotron infrared spectroscopy of OH-chondrodite and OH-clinohumite at high pressure. Am Mineral 88:1412-1415

Losos Z, Beran A (2004) OH defects in cassiterite. Mineral Petrol 81:219-234

Lu R, Keppler H (1997) Water solubility in pyrope to 100 kbar. Contrib Mineral Petrol 129:35-42

Maldener J, Rauch F, Gavranic M, Beran A (2001) OH absorption coefficients of rutile and cassiterite deduced from nuclear reaction analysis and FTIR spectroscopy. Mineral Petrol 71:21-29

Maldener J, Hösch A, Langer K, Rauch F (2003) Hydrogen in some natural garnets studied by nuclear reaction analysis and vibrational spectroscopy. Phys Chem Minerals 30:337-344

Martin RF, Donnay G (1972) Hydroxyl in the mantle. Am Mineral 57:554-570

Matsyuk SS, Langer K (2004) Hydroxyl in olivines from mantle xenoliths in kimberlites of the Siberian platform. Contr Mineral Petrol 147:413-437

Matsyuk SS, Langer K, Hösch A (1998) Hydroxyl defects in garnets from mantle xenoliths in kimberlites of the Siberian platform. Contr Mineral Petrol 132:163-179

Matveev S, O'Neill HSC, Ballhaus C, Taylor WR, Green DH (2001) Effect of silica activity on OH^- IR spectra of olivine: Implication for low-α-SiO_2 mantle metasomatism. J Petrol 42:721-729

Matveev S, Portnyagin M, Ballhaus C, Brooker R, Geiger CA (2005) FTIR spectrum of phenocryst olivine as an indicator of silica saturation in magmas. J Petrol 46:603-614

Miller GH, Rossman GR, Harlow GE (1987) The natural occurrence of hydroxide in olivine. Phys Chem Minerals 14:461-472

Mosenfelder JL (2000) Pressure dependence of hydroxyl solubility in coesite. Phys Chem Minerals 27:610-617

Mosenfelder JL, Schertl H-P, Smyth JR, Liou JG (2005) Factors in the preservation of coesite: The importance of fluid infiltration. Am Mineral 90:779-789

Mosenfelder JL, Deligne NI, Asimow PD, Rossman GR (2006) Hydrogen incorporation in olivine from 2-12 GPa. Am Mineral 91:285-294

Nasdala L, Beran A, Libowitzky E, Wolf D (2001) The incorporation of hydroxyl groups and molecular water in natural zircon ($ZrSiO_4$). Am J Sci 301:831-857

Nasdala L, Zhang M, Kempe U, Panczer G, Gaft M, Andrut M, Plötze M (2003) Spectroscopic methods applied to zircon. Rev Mineral Geochem 53:427-467

Ohtani E (2005) Water in the mantle. Elements 1:25-30

Ohtani E, Mizobata H, Yurimoto H (2000) Stability of dense hydrous magnesium silicate phases in the systems Mg_2SiO_4-H_2O and $MgSiO_3$-H_2O at pressures up to 27 GPa. Phys Chem Minerals 27:533-544

Paterson MS (1982) The determination of hydroxyl by infrared absorption in quartz, silicate glasses and similar materials. Bull Minéral 105:20-29

Pawley AR, McMillan PF, Holloway JR (1993) Hydrogen in stishovite, with implications for mantle water content. Science 261:1024-1026

Rossman GR (1990) Hydrogen in "anhydrous" minerals. Nucl Instr Meth Phys Res B45:41-44

Rossman GR (2006) Analytical methods for measuring water in nominally anhydrous minerals. Rev Mineral Geochem 62:1-28

Rossman GR, Aines RD (1986) Spectroscopy of a birefringent grossular from Asbestos, Quebec, Canada. Am Mineral 71:779-780

Rossman GR, Aines RD (1991) The hydrous components in garnets: Grossular-hydrogrossular. Am Mineral 76: 1153-1164

Rossman GR, Smyth JR (1990) Hydroxyl contents of accessory minerals in mantle eclogites and related rocks. Am Mineral 75: 775-780

Rossman GR, Beran A, Langer K (1989) The hydrous component of pyrope from the Dora Maira Massif, Western Alps. Eur J Mineral 1:151-154

Rossman GR, Rauch F, Livi R, Tombrello TA, Shi CR, Zhou ZY (1988) Nuclear reaction analysis of hydrogen in almandine, pyrope, and spessartite garnets. N Jb Miner Mh 1988:172-178

Skogby H (1999) Water in nominally anhydrous minerals. *In:* Microscopic Properties and Processes in Minerals. Wright K, Catlow R (eds) NATO Science Series, Kluwer Acad Publishers, p 509-522

Skogby H (2006) Water in natural mantle minerals I: pyroxenes. Rev Mineral Geochem 62:155-167

Skogby H, Halenius U (2003) An FTIR study of tetrahedrally coordinated ferrous iron in the spinel-hercynite solid solution. Am Mineral 88:489-492

Smyth JR, Holl CM, Frost DJ, Jacobsen SD, Langenhorst F, McCammon CA (2003) Structural systematics of hydrous ringwoodite and water in Earth's interior. Am Mineral 88:1402-1407

Snyder GA, Taylor LA, Jerde EA, Clayton RN, Mayeda TK, Deines P, Rossman GR, Sobolev NV (1995) Archean mantle heterogeneity and the origin of diamondiferous eclogites, Siberia: Evidence from stable isotopes and hydroxyl in garnet. Am Mineral 80:799-809

Song S, Zhang L, Chen J, Liou JG, Niu Y (2005) Sodic amphibole exsolutions in garnet from garnet-peridotite, North Qaidam UHPM belt, NW China: Implications for ultradeep-origin and hydroxyl defects in mantle garnets. Am Mineral 90:814-820

Swope RJ, Smyth JR, Larson AC (1995) H in rutile-type compounds: I. Single-crystal neutron and X-ray diffraction study of H in rutile. Am Mineral 80:448-453

Vlassopoulos D, Rossman GR, Haggerty SE (1993) Coupled substitution of H and minor elements in rutile and the implications of high OH contents in Nb- and Cr-rich rutile from the upper mantle. Am Mineral 78: 1181-1191

Wang L, Zhang Y, Essene EJ (1996) Diffusion of the hydrous component in pyrope. Am Mineral 81:706-718

Wieczorek A, Libowitzky E, Beran A (2004) A model for the OH defect incorporation in kyanite based on polarised IR spectroscopic investigations. Schweiz Min Petr Mitt 84:333-343

Withers AC, Wood BJ, Carroll MR (1998) The OH content of pyrope at high pressure. Chem Geol 147:161-171.

Woodhead JA, Rossman GR, Thomas AP (1991) Hydrous species in zircon. Am Mineral 76:1533-1546

Zhao Y-H, Ginsberg SB, Kohlstedt DL (2004) Solubility of hydrogen in olivine: dependence on temperature and iron content. Contrib Mineral Petrol 147:155-161